Available online at www.sciencedirect.com
ScienceDirect
Biochimica et Biophysica Acta 1767 (2007) 965–973
Biochimica et Biophysica Acta
BBA
www.elsevier.com/locate/bbabio

Functional roles of arginine residues in mung bean vacuolar H^+-pyrophosphatase

Yi-Yuong Hsiao [a,b], Yih-Jiuan Pan [a], Shen-Hsing Hsu [a], Yun-Tzu Huang [a], Tseng-Huang Liu [a], Ching-Hung Lee [a], Chien-Hsien Lee [a], Pei-Feng Liu [a], Wen-Chi Chang [a], Yung-Kai Wang [a], Lee-Feng Chien [c,1], Rong-Long Pan [a,*,1]

[a] *Department of Life Sciences and Institute of Bioinformatics and Structural Biology, College of Life Sciences, National Tsing Hua University, Hsin Chu 30043, Taiwan*
[b] *Department of Planning and Research, National Museum of Marine Biology and Aquarium, Pingtung, 94450, Taiwan*
[c] *Department of Life Sciences, College of Life Sciences, National Chung Hsing University, Tai Chung 40227, Taiwan*

Received 6 February 2007; received in revised form 26 April 2007; accepted 27 April 2007
Available online 3 May 2007

Abstract

Plant vacuolar H^+-translocating inorganic pyrophosphatase (V-PPase EC 3.6.1.1) utilizes inorganic pyrophosphate (PP_i) as an energy source to generate a H^+ gradient potential for the secondary transport of ions and metabolites across the vacuole membrane. In this study, functional roles of arginine residues in mung bean V-PPase were determined by site-directed mutagenesis. Alignment of amino-acid sequence of K^+-dependent V-PPases from several organisms showed that 11 of all 15 arginine residues were highly conserved. Arginine residues were individually substituted by alanine residues to produce R→A-substituted V-PPases, which were then heterologously expressed in yeast. The characteristics of mutant variants were subsequently scrutinized. As a result, most R→A-substituted V-PPases exhibited similar enzymatic activities to the wild-type with exception that R242A, R523A, and R609A mutants markedly lost their abilities of PP_i hydrolysis and associated H^+-translocation. Moreover, mutation on these three arginines altered the optimal pH and significantly reduced K^+-stimulation for enzymatic activities, implying a conformational change or a modification in enzymatic reaction upon substitution. In particular, R242A performed striking resistance to specific arginine-modifiers, 2,3-butanedione and phenylglyoxal, revealing that Arg^{242} is most likely the primary target residue for these two reagents. The mutation at Arg^{242} also removed F^- inhibition that is presumably derived from the interfering in the formation of substrate complex Mg^{2+}–PP_i. Our results suggest accordingly that active pocket of V-PPase probably contains the essential Arg^{242} which is embedded in a more hydrophobic environment.

Keywords: Proton translocation; Tonoplast; Vacuole; Site-directed mutagenesis; Vacuolar H^+-pyrophosphatase

1. Introduction

The plant vacuole is a multi-functional organelle for cellular homeostasis and embryonic development [1]. A membrane-associated vacuolar H^+-pyrophosphatase (V-PPase; EC 3.6.1.1) generates an H^+-electrochemical potential that motivates secondary transport of ions or metabolites across the vacuole membrane [2,3]. Several homologues of V-PPases have been found in archae, eubacteria, eukarya, and prokarya [4,5]. For years, V-PPases from various sources have been successfully purified and characterized as a 64–91 kDa homodimeric protein consisting of a single type of polypeptide with 660–793 amino acid residues and 14–17 putative transmembrane segments [1,4,6–11]. V-PPase contains several conserved motifs in cytoplasmic loops as functional domains for PP_i hydrolysis and free Mg^{2+} binding [3,12].

Abbreviations: BD, 2, 3-Butanedione; DDT, dithiothreitol; EGTA, ethyleneglycol-bis (β-aminoethylether); *N,N,N′,N′*, tetraacetic acid; PGO, Phenylglyoxal; PMSF, phenylmethylsulfonyl fluoride; V-PPase, vacuolar H^+-pyrophosphatase

* Corresponding author. Tel./fax: +886 3 5742688.
E-mail address: rlpan@life.nthu.edu.tw (R.-L. Pan).
[1] Contributed equally.

0005-2728/$ - see front matter © 2007 Elsevier B.V. All rights reserved.
doi:10.1016/j.bbabio.2007.04.007

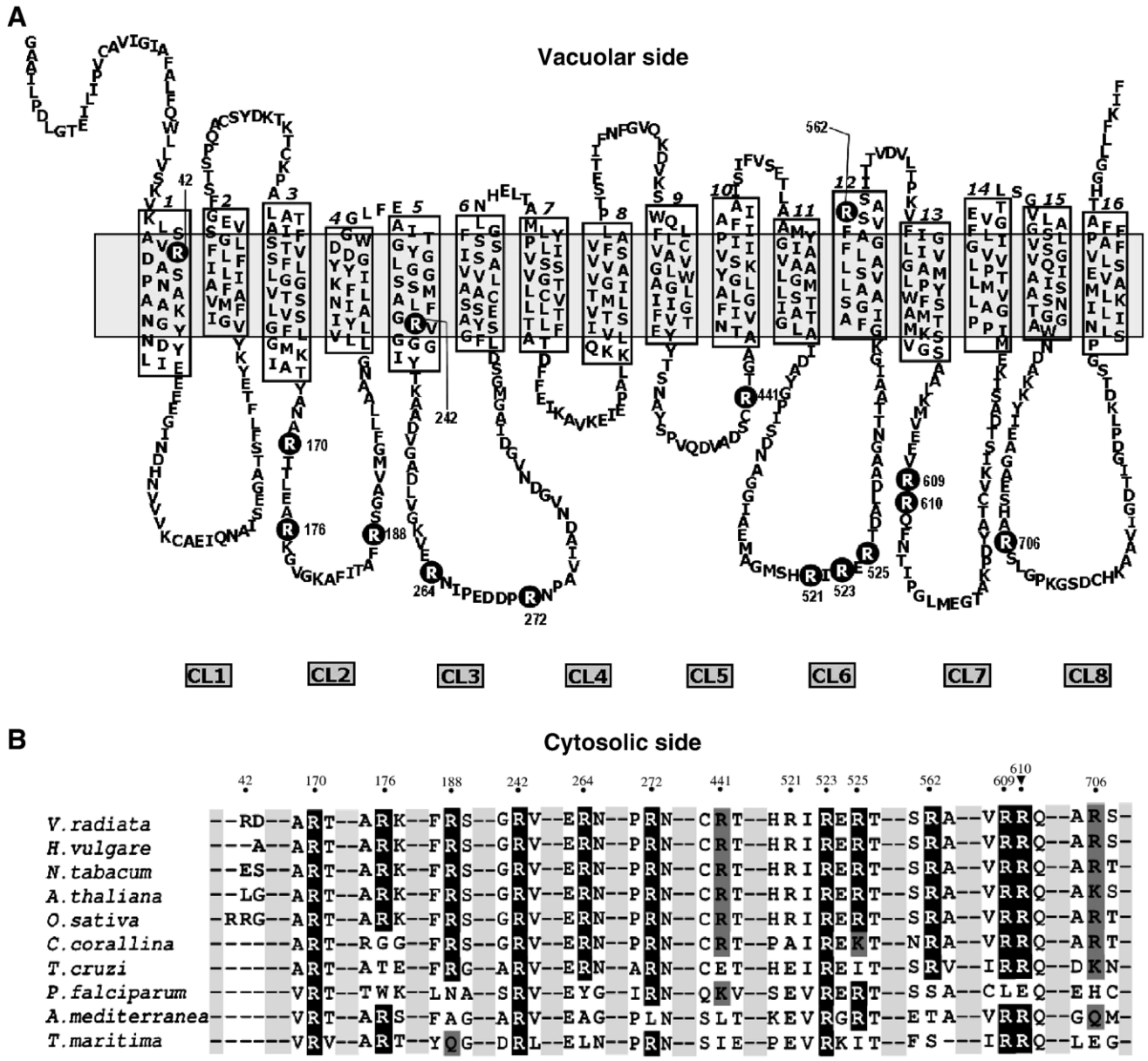

Fig. 1. The membrane topology and alignment of amino acid sequence of mung bean V-PPase. (A) Membrane topology model of V-PPase. This predicted model of mung bean V-PPase was modified from Nakashini et al. [9] and Mimura et al. [10]. The 16 transmembrane segments are boxed and 8 cytoplasmic loops (CL) are indicated below. The 15 Arg residues are specified by black circles with positions along amino acid sequence. (B) Alignment of amino acid sequence. The alignment of amino acid sequence of the fragments containing Arg was performed using the CLUSTAL W program [41]. The residue number of the alignment represents the location of Arg residues in *Vigna radiata* V-PPases. The residues in black shaded boxes stand for the identical (homology > 70%) residues in the alignment, in gray shaded boxes the highly similar (homology > 50%) residues, and in blank the low similarity regions (homology ≤ 50%), respectively. Dashes denote gaps in the sequence. The accession numbers of V-PPases from various sources are shown as follows: *Vigna radiata*,BAA23649; *Hordeum vulgare*, BAA02717; *Nicotiana tabacum*, CAA58701; *Arabidopsis thaliana*, BAA32210; *Oryza sativa*, BAA08232; *Chara coralline*, BAA36841; *Trypanosoma cruzi*, AAF80381; *Plasmodium falciparum*, AAD17215; *Acetabularia mediterranea*, BAA83103; *Thermotoga maritima*, D72409.

Regarding stimulation of the enzymatic activities by millimolar K^+, and the phylogenetic sequence of GNTTA/KE, two isoforms of V-PPase have been distinguished to be K^+-dependent and K^+-independent [4,11]. K^+-dependent V-PPase has been found in alga [13], protozoan [14], and most higher plants [15–17]. On the other hand, K^+-independent V-PPase exists in archaebacterium [18], photosynthetic bacterium [8], fungus [10], and *Arabidopsis thaliana* (AVP2) [18]. Moreover, some ions exert effects on the enzymatic activity of V-PPase; for instance, Ca^{2+}, Na^+, and F^- may substantially inhibit the enzyme [2,15,19]. Very recently, the importance of plant V-PPase has been addressed because of its linkage to stress-tolerance by altering the uptake of water and ions, and to organ development by regulating auxin transport [20–22]. Notwithstanding, the exact binding domain of these ions in this marvelous H^+-pumping enzyme remains to be determined.

Chemical modification and site-directed mutagenesis have been employed to reveal the functional requisite of amino acids in

Table 1
A list of oligonucleotides used for the R→A substitution of mung bean V-PPase

Name	Primer sequence
R42A	5′-GAGAAGCGTCTGCGACGGCAGAGAG-3′
R170A	5′-CTTACGCCAATGCAGCAACCACCCTGG-3′
R176A	5′-CACCCTGGAGGCAGCAAAGGGTGTTGG-3′
R188A	5′-CATTACGGCTTTTGCATCTGGTGCTGTTATG-3′
R242A	5′-TTCGGAGCAGTTGGCGGA-3′
R264A	5′-GGCAAGGTTGAGGCAAACATTCCCGAAG-3′
R272A	5′-GAAGATGATCCAGCAAATCCAGGTGTG-3′
R441A	5′-GCACCAGTTGCGCAGGAGTCAG-3′
R521A	5′-CTCACGAATTGCGTGACTCATG-3′
R523A	5′-CAGTTCTCTCAGCAATTCTGTGAC-3′
R525A	5′-GGCATCAGTTGCCTCACGAATTC-3′
R562A	5′-GTAATAGATGCTGCGCTCACAAAG-3′
R609A	5′-GAGGAAGTGGCCAGGCAATTC-3′
R610A	5′-GAAGTGCGCGCGCAATTCCAATAC-3′
R706A	5′-CTGAGCAGCATGCCGCAAGCCTTGG-3′
*Hin*dIII	5′-AAGCTTCAAAAAATGGGAGCAGCG-3′
*Xba*I	5′-CTCAACTCTCTAGAAGATCTTGAAGAG-3′
PRU-2028	5′-TCTATGGTTTCTAGGTCGCCTC-3′
PRF-1200	5′-CACTATCTTCAATTTTGGAGTGCA-3′
PRU-1000	5′-GGTGTCTTGACTGTTACTCTC-3′

The nucleotides of various primers for substitution are blocked in gray. Underlining indicates the addition of a new restriction cutting sites.

V-PPase. Evidence has shown that three DCCD-binding acidic residues Asp^{283}, Glu^{301}, and Asp^{500} of mung bean V-PPase are essential residues in or near the catalytic domain of the enzyme [12,23]. A substrate-protectable Cys^{634} of *Arabidopsis* V-PPase is reported to be critical for H^+-translocating reaction [24]. Site-directed mutagenesis of Lys^{261} and Glu^{263} of mung bean V-PPase demonstrated that these two residues probably play important roles in the energy conversion from PP_i hydrolysis to H^+-translocation [9]. In addition, various Asp residues confer to the binding of the substrate Mg^{2+}–PP_i complex [9]. Furthermore, mutation at Ala^{460} of thermophilic bacterium *Carboxydothermus hydrogenoformans* V-PPase could switch K^+-dependent enzyme to be K^+-independent [25]. Hsiao et al. [26,27] illustrated that His^{716} of mung bean V-PPase is a major target residue for diethylpyrocaronate inhibition. A mutation at the GYG/229–231 motif in transmembrane segments markedly depressed the enzymatic activities of PP_i hydrolysis, H^+-translocation, and coupling efficiency [28].

Our previous study indicated that mung bean V-PPase contains likely one essential Arg residue rendering the inhibition of its enzymatic activity and PP_i-dependent H^+-translocation by Arg specific chemical modifiers, such as phenylglyoxal (PGO) and 2, 3-butanedione (BD) [29]. Tuominen et al. [30] later found that Arg^{78} is involved in coordinating substrate PP_i binding at active sites in soluble PPase. Furthermore, mutagenic analysis on pyrophosphate synthase/pyrophosphatase from *Rhodospirillum rubrum* suggests that R176K mutants exhibit an increased salt tolerance [31]. Besides, Arg residues have been shown to play a crucial role not only in PPase but also in several types of ATPases. For instance, a P-type H^+-ATPase (AHA2), Arg^{655} is required for the ion coordination in the mechanism of H^+-translocating [32]. A substitution of Arg^{573} with Glu, Leu, or Gln in vacuolar Na^+-ATPase abolishes Na^+ transport and Na^+-stimulated ATP hydrolysis of the enzyme [33]. It was also indicated that the substitution of Arg^{282} with a Glu residue in the H^+-peptide co-transporter (PepT1) seemingly changes it from an H^+-driven to a facilitated transporter for peptides [34]. All these findings on ATPase and PPase imply that the Arg residue is highly involved in ionic substrate binding, H^+-translocation, and coupling mechanism of transporters.

Transmembrane topology analysis predicts mung bean V-PPase consists of 16 transmembrane segments with a putative substrate binding motif (DX_7KXE/253–263) in cytoplasmic loop 3 (CL3) and two acidic motifs (DX_3DX_3D/279–287 and /723–731) in CL3 and CL8, respectively (Fig. 1A) [3,9]. Furthermore, 11 residues of 15 Arg are highly conserved in K^+-dependent V-PPase as determined from analysis on amino acid sequence from several organisms (Fig. 1B). Meanwhile, the proposed topological structure suggests that 12 Arg among the 15 Arg residues of the mung bean V-PPase are located in the cytoplasmic loops and the remaining 3 Arg on the transmembrane segments, respectively. The exact roles of these Arg residues in V-PPase are yet to be determined.

In this study, functional roles of Arg residues in mung bean V-PPase were investigated using site-directed mutagenesis. We further demonstrated the Arg^{242} is primarily the target of PGO and BD inhibition and presumably is embedded in a more hydrophobic environment at active site of V-PPase.

2. Materials and methods

2.1. Microorganism and plasmids

The *E. coli* strain XL1-Blue (*recA1, endA1, gyrA96, thi-1, hsdR17, supE44, relA1, lac [F′ proAB, lacI^{q}ZΔM15*, Tn10 (Tet^r)]) was used as the host for DNA preparation and mutagenesis. The *Saccharomyces cerevisiae* strain BJ2168 (*MATa, prc1-407, prb1-1122, pep4-3, leu2, trp1, ura3-52*) was utilized as a host for heterologous expression of the enzyme [27,35]. BJ2168 was grown in YEPD medium [1% (w/v) yeast extract, 2% (w/v) peptone, and 2% (w/v) dextrose at pH 5.5]. The full-length cDNA of mung bean (*Vigna radiata* L. TN5) V-PPases was inserted into the multiple-cloning site between *Hin*dIII and *Xba*I after the *GAL1* promoter. The yeast transformation was performed by the LiAc/PEG method [36]. The plasmid DNA was extracted using a Gene-Spin™ DNA extraction kit (Protech Technology, Taiwan).

2.2. Mutagenesis and expression of R→A substituted V-PPase in yeast cells

Each substitution was carried out by the PCR megaprimer method [37] using two flanking primers and a mutagenic oligonucleotide as listed in Table 1. The Arg codon was replaced by an Ala codon in mutagenic oligonucleotides. The desired mutation was verified by DNA sequencing. The pYES2 plasmids from the vector alone, wild type, and R→A-substituted mutants were transformed into yeast BJ2168. The transformed yeast cells were selected on CM plates [0.5% (w/v) ammonium sulfate, 2% (w/v) glucose, 0.2% (w/v) yeast nitrogen base without amino acid, 2.0% (w/v) Bacto agar, and supplemented with 60 μg/ml leucine and 60 μg/ml tryptophan but without uracil (as a selection marker)].

2.3. Preparation of yeast microsmomes containing R→A substituted V-PPase

Yeast microsomal preparation was performed as described previously with minor modifications [27,35]. The transformed yeast cells were grown in 400 ml of CM medium at 30 °C. When grown to 1×10^7 cells/ml, the cells were harvested by centrifugation at 4000×*g* for 10 min. The cell pellets were then

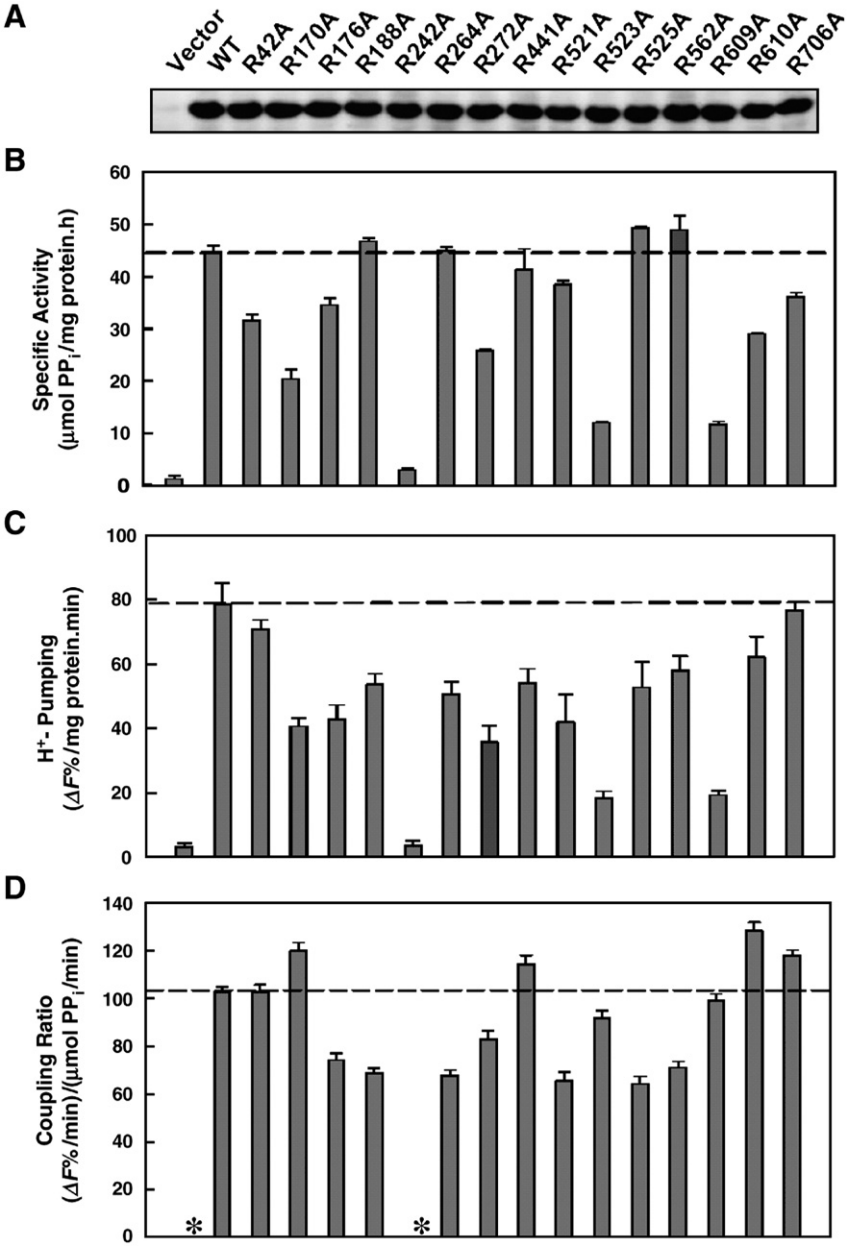

Fig. 2. Expression and activity assay of R→A-substituted V-PPases. (A) The expression level shown by western blot. (B) PP_i hydrolysis activity. (C) PP_i-dependent H^+-translocation. (D) Coupling ratio. The coupling ratio of variant R→A-substituted V-PPases were determined as described under Materials and methods. Fifteen μg microsomal proteins were loaded on each lane. Values are means±S.D. from at least 3 independent experiments. Asterisks (*) represent data unable to be calculated.

suspended in l liter of CM medium containing 2% (w/v) galactose and incubated at 30 °C for 3 days. As the A_{600} of medium reached 1.0, the cells were harvested by centrifugation at 4000×*g* for 10 min. The yeast cell pellets were washed with ddH_2O, resuspended with wash buffer [100 mM Tris–HCl (pH 9.4) and 10 mM DTT], and incubated at 37 °C for 20 min with gentle shaking. The cells were centrifuged again and resuspended in 100 ml of YP medium [100 mM Tris–Mes (pH 7.6), 1% (w/v) yeast extract, 2% (w/v) peptone, 1% (w/v) galactose or glucose, 0.7 M sorbitol, and 5 mM DTT]. The cell suspension was then added with 1,200 U lyticase per g wet weight of yeast pellets and incubated at 30 °C for 2 h with gentle shaking to generate the spheroplasts. Yeast spheroplasts were collected by centrifugation at 4000×*g* for 10 min and resuspended in an ice-cold homogenization buffer [50 mM Tris–ascorbate (pH 7.6), 5 mM EGTA–Tris, 10% (w/v) glycerol, 2 mg/ml BSA, 1.5% (w/v) polyvinylpyrrollidone (M_r 40,000), 1 mM PMSF, 10 μg/ml pepstatin A, and 10 μg/ml leupetin]. The suspension was subjected to a Dounce glass homogenizer by 20 strokes with a tight fitting pestle. The homogenate was centrifuged at 1000×*g* for 10 min to remove cellular debris and unbroken cells. The supernatant was carefully aspirated and centrifuged at 84,000×*g* for 1 h to harvest the microsomal membrane fraction. The pellets were resuspended in suspension buffer [5 mM Tris–Mes (pH 7.6), 1 mM EGTA–Tris, 1.1 M glycerol, 2 mg/ml BSA, 2 mM DTT, 1 mM PMSF, and 10 μg/ml pepstatin A], and carefully layered on the 10% (w/w) and 28% (w/w) of discontinuous sucrose density gradient, followed by centrifugation at 58,000×*g* for 2 h. The membrane fractions that retained V-PPases at the interface of the sucrose gradients of 10% and 28% (w/w) were collected. The membrane fractions were then washed with 10 volumes of storage buffer [5 mM Tris–Mes (pH 7.6) and 10% (w/v) glycerol] and centrifuged at 84,000×*g* for 55 min. Finally the membrane pellets were suspended in the storage buffer and stored at −80 °C for later use. Protein concentrations were measured using the Bradford protein assay reagent (Bio-Rad, Hercules, CA, USA) while BSA was employed as the standard [38].

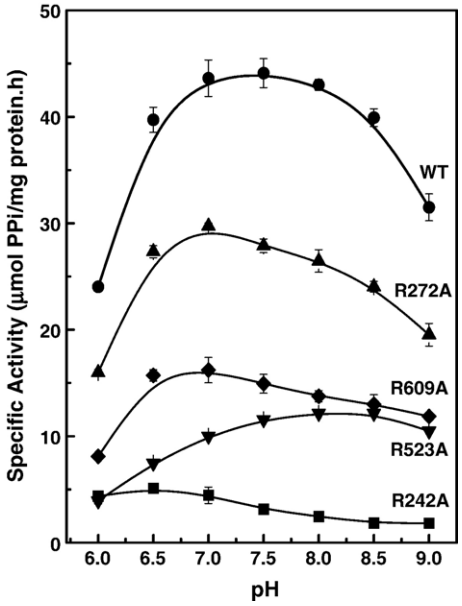

Fig. 3. The pH profiles for PPi hydrolysis of R→A-substituted V-PPases. The optimal pH for PP_i hydrolysis activity of variant R→A-substituted V-PPase was measured as described under Materials and methods. The pH values of reaction mixtures were adjusted using Tris–Mes buffer. The symbols represent: (●), WT; (■), R242A; (▲), R272A; (▼), R523A; (♦), R609A. Values are means ±S.D. from at least 3 independent experiments.

2.4. Assay of PP_i hydrolysis activity of V-PPase

The PP_i hydrolysis activity of V-PPase was determined as the rate of P_i liberation. Fifteen to thirty μg of microsomal proteins were incubated with reaction medium [30 mM Tris–Mes (pH 8.0), 1 mM Na_4PP_i, 1 mM $MgSO_4$, 50 mM KCl, 0.5 mM NaF, and 1.5 μg/ml gramicidin D] at 37 °C for 15–20 min. The PP_i hydrolysis reaction of V-PPase under the routine conditions is in a linear function at the time period. The enzymatic reaction of V-PPase was terminated by the stop solution [1.7% (w/v) ammonium molybdate, 2% (w/v) SDS, and 0.02% (w/v) 1-amino-2-naphthol-4-sulphonic acid] and the released P_i measured spectrophotometrically [39]. To determine the optimal pH for enzymatic activities of various R→A substituted V-PPases, the pH values of reaction mixtures were adjusted by Tris–Mes buffer.

2.5. Measurement of H^+-translocation of V-PPase

The proton translocation by microsomal vesicles was observed as the fluorescence quenching of acridine orange (excitation wavelength 495 nm, emission wavelength 530 nm) using a Hitachi F-4000 fluorescence spectrophotometer (Hitachi Ltd., Tokyo, Japan). The H^+-translocating reaction was measured in the medium containing 5 mM Tris–HCl (pH 7.6), 1 mM EGTA–Tris, 400 mM glycerol, 100 mM KCl, 1.3 mM $MgSO_4$, 0.5 mM NaF, 5 μM acridine orange, and 150–200 μg microsomal proteins. The fluorescence quenching was initiated by adding 1 mM Na_4PP_i (pH 7.6) and the initial quench rate was calculated as the proton transport activity [27,28]. The ionophore, gramicidin D (5 μg/ml), was added at the end of each assay to confirm the integrity of the membrane. Apparent coupling ratio (the ratio of initial proton pumping rate to that of PP_i hydrolysis) was measured as (ΔF%/min)/(μmol PP_i hydrolyzed/min) according to Zhen et al. [12].

2.6. SDS-PAGE and western blot analysis

Sodium dodecyl sulfate-polyacrylamide gel electrophoresis (SDS-PAGE) was performed as described by Laemmli [40]. Proteins of membrane fractions containing R→A-substituted V-PPases were separated on a 10% (w/v) SDS-PAGE, and visualized with coomassie blue staining or transferred to polyvinylidene difluoride (PVDF) membranes using a semi-dry Nova Blot apparatus (Amersham Pharmacia Biotech, now GE Healthcare, Buckinghamshire, UK). Western blot analysis was carried out utilizing the primary antibody against the KLH-conjugated synthetic polypeptide of a hydrophilic loop sequence (KVERNIPEDDPRNPA/261–275) from mung bean V-PPases. The antibody was purified using a Protein G Sepharose column (Amersham Pharmacia Biotech, now GE Healthcare, Buckinghamshire, UK). The blot was stained and visualized by the Western Lightning™ kit (New England Nuclear, now PerkinElmer Life Sciences Inc., Boston, USA).

2.7. Chemical modification of V-PPase by phenylglyoxal (PGO) and 2, 3-butanedione (BD)

The R→A-substituted V-PPases were incubated with 50 mM PGO in a reaction buffer containing 25 mM Mops–KOH (pH 7.9) or with 200 mM BD in 25 mM borate–KOH (pH 7.9) at 37 °C for 10 min, respectively. The reaction was stopped by dilution with 25 volumes of PP_i hydrolysis assay medium [30 mM Tris–Mes (pH 8.0), 1 mM $MgSO_4$, 0.5 mM NaF, 50 mM KCl, 1 mM PP_i, and 1.5 μg/ml gramicidin D] and PP_i liberation measured immediately.

2.8. Trypsin proteolysis assay

The microsomal membrane proteins of R→A-substituted V-PPase (15 μg) were incubated with TPCK-treated trypsin at a protein ratio of 100:1 (w/w) at 37 °C for 20 min. The proteolysis reaction was stopped by directly adding SDS-PAGE sample buffer [cf., 40] followed by immediate heating at 95 °C for 5 min. The V-PPase was visualized upon 10% (w/v) SDS-PAGE and western blot analysis as described above.

2.9. Determination of the background concentration of K^+, Na^+, and Ca^{2+} in assay media

The concentrations of K^+, Na^+, and Ca^{2+} in the reaction media [30 mM Tris-Mes (pH 8.0)] were determined by Inductively Coupled Plasma Mass Spectrometry (ICP-MS) at NTHU Instrument Center, National Tsing Hua University, Hsin Chu, Taiwan.

Table 2
Cation effects on the PPi hydrolysis activity of R→A substituted V-PPases

Mutants	K^+-stimulation (fold)	Na^+ inhibition (%)	Ca^{2+} inhibition (%)
WT	8.2±0.9	39.0±6.4	65.3±1.2
R42A	9.0±0.2	24.4±1.4	63.2±2.0
R170A	6.2±0.6	27.5±3.0	64.2±2.0
R176A	8.3±0.5	43.7±3.8	69.1±1.0
R188A	7.6±0.4	40.1±2.3	56.7±0.1
R242A	1.4±0.1	33.7±8.8	69.7±3.1
R264A	5.6±0.9	29.5±9.4	70.6±3.0
R272A	4.7±0.4	43.4±4.1	68.6±0.5
R441A	10.8±0.3	22.4±2.1	61.2±2.0
R521A	7.2±0.7	39.2±6.6	66.1±1.9
R523A	4.4±0.2	25.3±4.3	55.3±5.3
R525A	8.4±0.5	40.1±3.8	67.3±1.3
R562A	6.9±0.6	52.4±3.8	60.7±2.3
R609A	4.0±0.6	24.8±11.4	57.6±3.7
R610A	6.0±0.8	50.8±6.2	60.8±3.5
R706A	8.1±0.3	23.5±3.9	60.5±2.3

The heterologously expressed R→A substituted V-PPases of microsomal membranes were prepared from *S. cerevisiae* as described under Materials and methods. The names of each mutant shown are Arg residues individually replaced by Ala. The ion concentrations: 50 mM K^+, 100 mM Na^+ and 0.1 mM Ca^{2+}. Values are means±S.D. from at least 3 separate experiments. The percentage inhibition is [(1−ratio of specific activities in the presence over in the absence of the ions interested)×100].

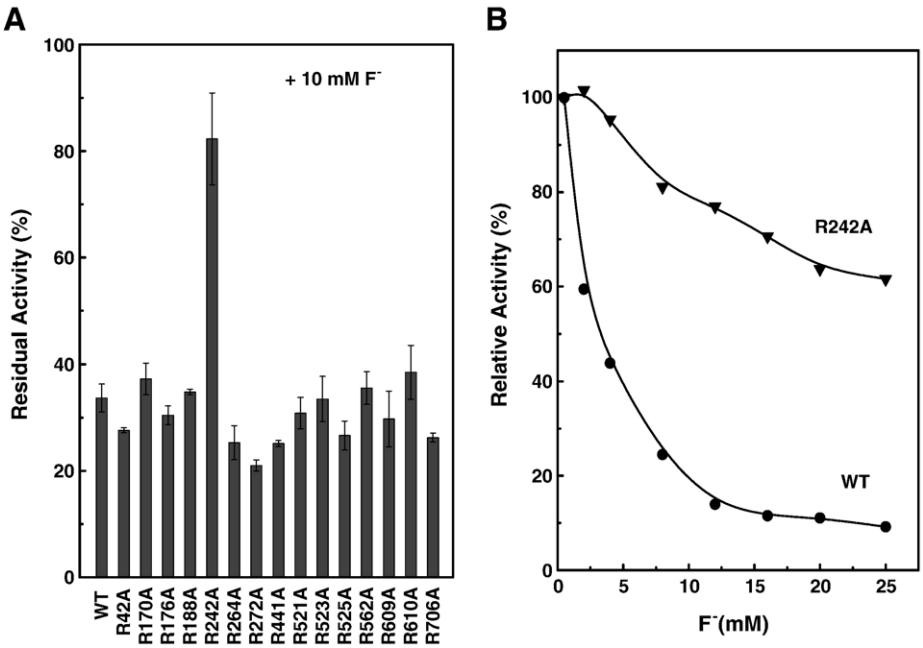

Fig. 4. Fluoride inhibition of R→A-substituted V-PPases. (A) Inhibition of the PPi hydrolytic activity of the V-PPases by F^-. (B) Concentration dependence of fluoride inhibition of the H^+-PPases. The PPase activity assay was performed with the reaction medium in the presence of 10 mM NaF as described under Materials and methods. Values are means±S.D. from at least 3 independent experiments. (●), WT; (▼), R242A. The control activities of the wild-type and R242A were 43.4±2.8 and 4.0±0.4 μmol PP_i/mg protein h.

2.10. Materials

Restriction enzymes and T_4 DNA ligase were purchased from New England Biolabs (Beverly, MA, USA) and lyticase from Sigma (St. Louis, MO, USA). All other chemicals were of analytic grade and used without further purification.

3. Results and discussion

3.1. Functional expression and characterization of the R→A-substituted V-PPase

Fig. 1 depicts 11 Arg residues corresponding to Arg^{170}, Arg^{176}, Arg^{188}, Arg^{242}, Arg^{264}, Arg^{272}, Arg^{523}, Arg^{525}, Arg^{562}, Arg^{609} and Arg^{610} are highly conserved in K^+-dependent V-PPases (Fig. 1B). Arg^{242} is accommodated in a conserved motif of RVGGGIYTK/242–250 in CL3, assigned to the substrate Mg^{2+} PP_i -binding sites (Fig. 1A) [9]. Three Arg residues, Arg^{521}, Arg^{523}, and Arg^{525}, closely reside on CL6, but their function remains to be identified. Twins of Arg^{609} and Arg^{610} were located in a conserved motif EVRRQ/607–611 in CL7, presumably a loop for conformational flexibility of V-PPase [8,11]. These 15 Arg residues were individually substituted by neutral Ala residue using a site-directed mutagenesis technique.

The cDNAs encoding mung bean V-PPases were transformed into the yeast vector pYES2 with *Gal1* as a promoter, and then heterologously expressed in a protease deficient yeast stain BJ2168. Microsomes with R→A-substituted V-PPase were successfully isolated from yeasts and the expression of each mutated enzyme was examined by western blotting. Fig. 2A depicts similar expression level of wild type and mutant V-PPases upon western blotting analysis. The PP_i hydrolysis of the wild type V-PPase was stimulated 5–7 fold by 30 mM K^+ [27]. However, most of the R→A-substituted V-PPases exhibited decreased PP_i hydrolysis activity at different levels compared to the wild type (Fig. 2B). In particular, the Arg^{242}→Ala (R242A) mutant almost completely lost PP_i hydrolysis activity. Both Arg^{523}→Ala (R523A) and Arg^{609}→Ala (R609A) variants held partial enzyme activity (<30%). On the other hand, Arg^{272}→Ala (R272A) and Arg^{170}→Ala (R170A) mutants displayed approximately one half of the wild type enzyme activity while the rest of them till retained at level of 70 to 110%. We also observed the PP_i-dependent H^+-translocation of wild type and mutant V-PPases (Fig. 2C). The R242A variant completely lost H^+-translocation ability while the R523A and R609A mutants partially maintained it at approximately 25% level (Fig. 2C). The remaining mutants showed 50–100% of H^+-translocating activities as compared to the wild type. We further calculated the coupling ratio by PP_i-dependent H^+-translocation over PP_i-hydrolysis activity. There was no significant difference in the coupling ratios between the wild type and mutants (Fig. 2D). These results indicated that the PP_i hydrolysis activity and H^+-translocation of R242A, R523A, and R609A mutants were concomitantly blocked while the rest of mutants maintained the capacities of wild-type V-PPase. It is conceivable that Arg^{242}, Arg^{523}, and Arg^{609} are probably involved in the V-PPase functions, locating presumably in/or at vicinity of its active pocket.

3.2. The optimal pH for enzymatic activity of the R→A-substituted V-PPases

The optimal pH values for the enzymatic activities of V-PPases from wild type and mutants are shown in Fig. 3. The

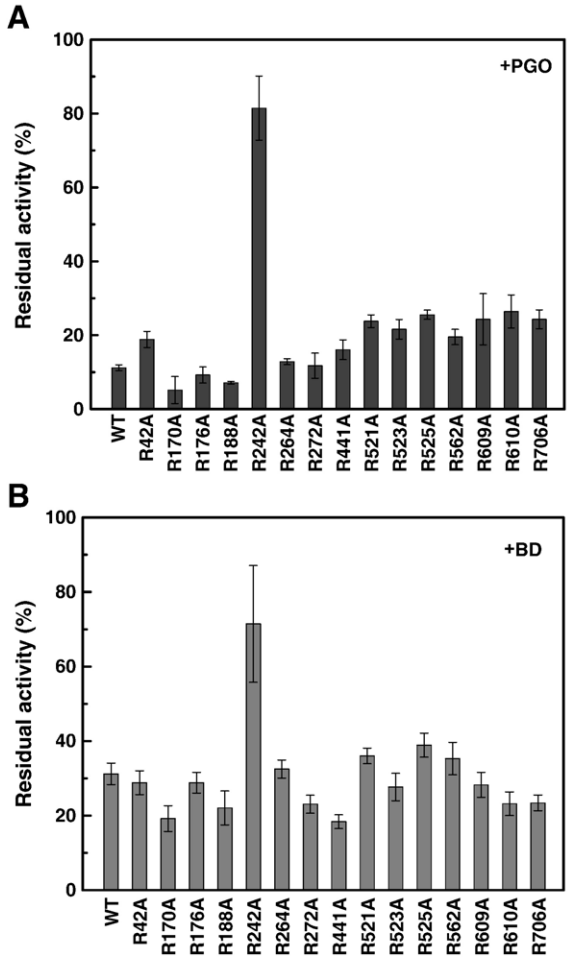

Fig. 5. Inhibition of R→A-substituted V-PPases by PGO and BD. (A) Inhibition of V-PPase by PGO. The PGO modification of membrane fractions containing R→A-substituted V-PPase was performed in the presence of 50 mM PGO. The assay was conducted as described under Materials and methods. (B) Inhibition of V-PPase by BD. The BD modification reactions were similarly performed in the presence of 200 mM BD. Relative residual activity (%) was calculated as the ratio of specific activity in the presence over in the absence of PGO or BD, respectively. Values are means±S.D. from at least 3 independent experiments. The control activities of the wild-type and R242A were 32.75±0.8 and 4.7±0.2 μmol PP_i/mg protein h.

optimal pH for the enzymatic activity of wild type V-PPase was at approximately pH 7.5. For mutants R242A, R272A and R609A, the optimal pH was shifted to an acidic range by 0.5–1.0 units as compared to the wild type. In contrast, the R523A revealed an optimal pH shift to basic by about 1.3 units. The other mutants maintained an optimal pH value similar in range to that of the wild type (data not shown).

It was reported that at least four ionizable groups are essential for the catalytic function of mung bean V-PPase: the groups at pKa 5.7 and 8.6 for substrate binding and those at pKa 6.1 and 9.0 in the substrate-conversion step [19]. Thus, Arg^{242}, Arg^{272}, Arg^{609}, all shifting optimal pH toward acidic upon mutation, and Arg^{523}, drafting toward basic range, are prominently the candidates for substrate binding and energy conversion of V-PPase. Notwithstanding, losing the positive charge of the Arg residue may provoke a conformational change, destabilizing the enzyme structure, or diminishing binding and conversing abilities of the enzyme–substrate complex of the V-PPase.

3.3. Ion effects on enzymatic activity of R→A-substituted V-PPase

The background ionic concentrations of reaction media [30 mM Tris–Mes (pH 8.0)] were determined respectively by ICP-MS to be: K^+<0.2 μM, Na^+<0.6 μM, and Ca^{2+}<1 μM, and considered suitable for the assay of ion effects in this work. The effects of ions on the wild type and mutants are summarized in Table 2. Mutants showed different degrees of stimulation by K^+. For instance, R42A and R441A displayed a slight increase in K^+-stimulation by 9.0 and 10.8-fold, respectively, as compared to 8.4-fold of the wild type. In contrast, those of R272A, R523A, and R609A were reduced to one half of the wild type. The K^+ stimulation of R242A was substantially decreased to be 1.4-fold. Mutation on the rest of arginine residues may partially relieve K^+-stimulation.

The exact K^+-binding site in V-PPase is not fully understood. Since the V-PPase of *C. hydrogenoformans* turns dramatically from a K^+-dependent into a K^+-independent type upon replacement of Ala^{460} by lysine, it is believed that Ala^{460} may possibly locate at K^+ binding site [25]. Our recent study also reveals that the C-terminal region of mung bean V-PPase probably contains the K^+ binding domain of the enzyme [41]. In this study, we further demonstrate that the R→A substitutions at Arg^{242}, Arg^{264}, Arg^{272}, Arg^{523} and Arg^{609} may partially alleviate K^+-stimulation. These residues are distributed in

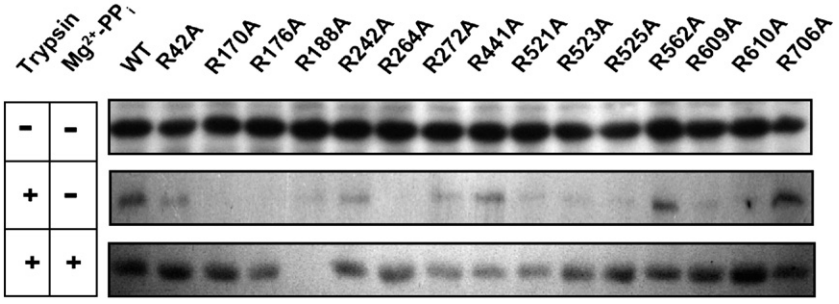

Fig. 6. Trypsinolysis analysis of R→A-substituted V-PPases. Microsomal membrane proteins (15 μg) were pre-incubated with TPCK-treated trypsin at a ratio of protein to trypsin 100:1 (w/w) at 37 °C for 20 min. The trypsin proteolysis mixtures (15 μg protein) were then loaded on gel for SDS-PAGE and western blot analysis as described under Materials and methods.

different functional domains of the mung bean V-PPase, suggesting that more than one segment or motif in the V-PPase are involved in the binding of K^+. In particular, the mutation of Arg^{242} seriously abolished K^+-stimulation of V-PPase, implying that Arg^{242} may play a more significant role in K^+-binding and/or stimulation of the enzymatic activity. Nevertheless, we cannot exclude the possibility of long-distance conformational disturbance upon substitution of these Arg residues.

It has been well known that Ca^{2+} and Na^+ could substantially inhibit V-PPase [2,3,15]. The inhibitory effects of Na^+ and Ca^{2+} inhibition on R→A substituted V-PPase were also investigated. The mutation at Arg residues exhibited various degree of Na^+ inhibition but not of Ca^{2+} inhibition (Table 2). For instance, R562A and R610A were more sensitive to Na^+ inhibition than R42A, R170A, R441A, R523A, R609A and R706A. Surprisingly, there is no effect upon the mutation at Arg^{242}, excluding its role in Na^+-inhibition. It is believed the binding of Na^+ seems more ubiquitous than at specific sites.

PP_i hydrolysis activities of the wild type and all mutants were inhibited by approximately 60% at 10 mM F^- except that of R242A by only 18% (Fig. 4A). Moreover, we examined the concentration dependence of F^- inhibition in the wild type and R242A variant. The wild type was inhibited significantly by F^- in a manner concomitant with the increase of F^- concentration, whereas the R242A mutant by a lesser degree. For instance, the enzymatic activity of R242A was inhibited by 40% at 25 mM F^- as compared to 90% of the wild type under similar conditions (Fig. 4B). Our work here suggested that Arg^{242} participates probably in F^- binding and/or locates in the vicinity of F^- binding site. Since F^- may exert the inhibition by interfering substrate complex Mg^{2+}–PP_i [15,42], it is conceivable that Arg^{242} resides presumably at the active site.

3.4. Identification of target residue for PGO and BD inhibition

We identified the Arg residues that may be involved in the PP_i hydrolysis of V-PPase by Arg group specific modifiers PGO and BD (Fig. 5). The PP_i hydrolysis reaction of wild type V-PPase was inhibited by 50 mM PGO to about 10% of the residual enzyme activity. The R→A-substituted V-PPases showed different sensitivities to the PGO. Most mutants exhibited approximately 15–30% of the residual enzyme activity while R170A, R176A, and R188A were even more sensitive to PGO than the wild type. In contrast, the R242A mutant showed relatively high resistance to PGO, remaining 80% of the residual enzyme activity. In addition, upon treatment with 200 mM BD, the wild type V-PPase maintained 30% of the residual enzyme activity. Likewise, all the R→A-substituted V-PPases exhibited similar sensitivities to BD, again except R242A, which retained about 70% of the residual enzyme activity. These analyses demonstrate that Arg^{242} is the major target of PGO and BD. Furthermore, it is shown V-PPases were more sensitive to PGO than to BD (Fig. 5). Since PGO is more hydrophobic than BD, it is reasonably suggested that Arg^{242} is probably embedded in a more hydrophobic environment.

3.5. Trypsinolysis of R→A-substituted V-PPases

To explore the structural integration and stability of V-PPase upon R→A-substitution, trypsin proteolysis and the protection effect of the substrate complex Mg^{2+}–PP_i were examined. The microsomal proteins were treated with trypsin in the absence and presence of Mg^{2+}–PP_i and then lysis visualized by immunoblotting, respectively (Fig. 6). In the absence of Mg^{2+}–PP_i complex, most V-PPase variants were completely digested by trypsin except minor residual proteins left for wild type, R42A, R242A, R441A, R562A, and R706A. Severe digestion implicates substantial accessibility of V-PPases to trypsin attack. However, in the presence of the substrate complex, considerable protection was provided, except for R188A, suggesting that the physiological substrate Mg^{2+}–PP_i may exert a rigid structure against the attack of trypsin. Nevertheless, R188A could be digested in spite of the presence or absence of substrate complex, indicating that the mutated Arg^{188} may directly or indirectly exposes the spot for trypsin cleavage.

Moreover, our data revealed that the R242A mutant is not significantly affected by the trypsin proteolysis in the absence or presence of the Mg^{2+}–PP_i complex. These results suggest that R→A substitution at R242 of V-PPase does not provoke seriously structural de-stability or conformational change, regardless the loss of PP_i hydrolysis and H^+-translocation activities (Figs. 2 and 6). Therefore, we speculate that Arg^{242}, presumably embedded in a hydrophobic region, may participate in the PP_i hydrolysis. This notion concurs with suggestion of Nakanish et al. [9] that mung bean V-PPase contains a functional motif of RVGGGIY/242–248 close to the PP_i binding domain in the TM5 segment. Furthermore, Mimura et al. [10] recently had also demonstrated this conserved motif in *S. coelicolor* V-PPase and predicted that it is inserted in a more hydrophobic region of the membrane. In addition, the Arg^{246} of *Arabidopsis thaliana*, equivalent to Arg^{242} of *Vigna radiata*, was found a functionally essential residue in both the PP_i hydrolysis and H^+-translocation reactions [43].

In summary, our work revealed that the active site of V-PPase probably contains an essential Arg^{242}, which confers the inhibition by group specific modification of PGO and BD and is embedded in a more hydrophobic environment. The detailed structure of the active pocket of V-PPase remains to be further elucidated.

Acknowledgements

This work was supported by the grants from the National Science Council, Taiwan to RLP (NSC94-2627-M-007-003 and NSC94-2311-B-007-012).

References

[1] M. Maeshima, Tonoplast transporters: organization and function, Annu. Rev. Plant Physiol. Plant Mol. Biol. 52 (2001) 469–497.
[2] P.A. Rea, J. Poole, Vacuolar H^+-translocating pyrophosphatase, Annu. Rev. Plant Physiol. Plant Mol. Biol. 44 (1993) 157–180.
[3] M. Maeshima, Vacuolar H^+-pyrophosphatase, Biochim. Biophys. Acta 1465 (2000) 37–51.

[4] Y.M. Drozdowicz, P.A. Rea, Vacuolar proton-pyrophosphatases: from the evolutionary backwaters into the mainstream, Trends Plant Sci. 6 (2001) 206–211.
[5] A. Serrano, J.R. Perez-Castineira, H. Baltscheffsky, M. Baltscheffsky, Proton-pumping inorganic pyrophosphatases in some archaea and other extremophilic prokaryotes, J. Bioenerg. Biomembranes 36 (2004) 127–133.
[6] M.H. Sato, M. Maeshima, Y. Ohsumi, M. Yoshida, Dimeric structure of H^+-translocating pyrophosphatase from pumpkin vacuolar membranes, FEBS Lett. 290 (1991) 177–180.
[7] C.J. Britten, R.G. Zhen, E.J. Kim, P.A. Rea, Reconstitution of transport function of vacuolar H^+-translocating inorganic pyrophosphatase, J. Biol. Chem. 267 (1992) 21850–21855.
[8] M. Baltscheffsky, A. Schultz, H. Baltscheffsky, H^+-PPases: a tightly membrane-bound family, FEBS Lett. 457 (1999) 527–533.
[9] Y. Nakanishi, T. Saijo, Y. Wada, M. Maeshima, Mutagenic analysis of functional residues in putative substrate-binding site and acidic domains of vacuolar H^+-pyrophosphatase, J. Biol. Chem. 276 (2001) 7654–7660.
[10] H. Mimura, Y. Nakanishi, M. Hirono, M. Maeshima, Membrane topology of the H^+-pyrophosphatase of *Streptomyces coelicolor* determined by cysteine-scanning mutagenesis, J. Biol. Chem. 279 (2004) 35106–35112.
[11] H. Mimura, Y. Nakanishi, M. Maeshima, Disulfide-bond formation in the H^+-pyrophosphatase of *Streptomyces coelicolor* and its implications for redox control and enzyme structure, FEBS Lett. 579 (2005) 3625–3631.
[12] R.G. Zhen, E.J. Kim, P.A. Rea, Acidic residues necessary for pyrophosphate-energized pumping and inhibition of the vacuolar H^+-pyrophosphatase by *N,N′*-dicyclohexylcarbodiimide, J. Biol. Chem. 272 (1997) 22340–22348.
[13] K. Takeshige, M. Tazawa, A. Hager, Characterization of the H^+ translocating adenosine triphosphatase and pyrophosphatase of vacuolar membranes isolated by means of a perfusion technique from *Chara corallina*, Plant Physiol. 86 (1988) 1168–1173.
[14] J.E. Hill, D.A. Scott, S. Luo, R. Docampo, Cloning and functional expression of a gene encoding a vacuolar-type proton-translocating pyrophosphatase from *Trypanosoma cruzi*, Biochem. J. 351 (2000) 281–288.
[15] M. Maeshima, H^+-translocating inorganic pyrophosphatase of plant vacuoles: inhibition by Ca^{2+}, stabilization by Mg^{2+} and immunological comparison with other inorganic pyrophosphatases, Eur. J. Biochem. 196 (1991) 11–17.
[16] Y.M. Drozdowicz, J.C. Kissinger, P.A. Rea, AVP2, a sequence-divergent, monovalent cation-insensitive H^+-translocating inorganic pyrophosphatase from *Arabidopsis thaliana*, Plant Physiol. 123 (2000) 353–362.
[17] Y. Sakakibara, H. Kobayashi, K. Kasamo, Isolation and characterization of cDNAs encoding vacuolar H^+-pyrophosphatase isoforms from rice (*Oryza sativa* L.), Plant Mol. Biol. 31 (1996) 1029–1038.
[18] Y.M. Drozdowicz, Y.P. Lu, V. Patel, S. Fitz-Gibbon, J.H. Miller, P.A. Rea, A thermostable vacuolar-type membrane pyrophosphatase from the archaeon *Pyrobaculum aerophilum*: implications for the origins of pyrophosphate-energized pumps, FEBS Lett. 460 (1999) 505–512.
[19] A.A. Baykov, N.P. Bakuleva, P.A. Rea, Steady-state kinetics of substrate hydrolysis by vacuolar H^+-pyrophosphatase. A simple three-state model, Eur. J. Biochem. 217 (1993) 755–762.
[20] J. Li, H. Yang, W.A. Peer, G. Richter, J. Blakeslee, A. Bandyopadhyay, B. Titapiwantakun, S. Undurraga, M. Khodakovskaya, E.L. Richards, B. Krizek, A.S. Murphy, S. Gilroy, R.A. Gaziola, Arabidopsis H^+-PPase AVP1 regulates auxin-mediated organ development, Science 310 (2005) 121–125.
[21] S. Park, J. Li, J.K. Pittman, G.A. Berkowitz, H. Yang, S. Undurraga, J. Morris, J.D. Hirschi, R.A. Gaziola, Up-regulation of a H^+-pyrophosphatase (H^+-PPase) as a strategy to engineer drought-resistant crop plants, Proc. Natl. Acad. Sci. U. S. A. 102 (2005) 18830–18835.
[22] S. Guo, H. Yin, X. Zhang, F. Zhao, P. Li, S. Chen, Y. Zhao, H. Zhang, Molecular cloning and characterization of a vacuolar H^+-pyrophosphatase gene, SsVP, from the halophyte *Suaeda salsa* and its overexpression increases salt and drought tolerance of Arabidopsis, Plant Mol. Biol. 60 (2006) 41–50.
[23] S.J. Yang, S.S. Jiang, S.Y. Kuo, S.H. Hung, M.H. Tam, R.L. Pan, Localization of a carboxylic residue possibly involved in the inhibition of vacuolar H^+-pyrophosphatase by *N,N′*-dicyclohexylcarbodiimide, Biochem. J. 342 (1999) 641–646.
[24] E.J. Kim, R.-G. Zhen, P.A. Rea, Site-directed mutagenesis of vacuolar H^+-pyrophosphatase: necessity of Cys^{634} for inhibition by maleimides but not catalysis, J. Biol. Chem. 270 (1995) 2630–2635.
[25] G.A. Belogurov, R.A. Lathi, Lysine substitute for K^+: A460K mutation eliminates K^+ dependence in H^+-pyrophosphatase of carboxydothermus hydrogenoformans, J. Biol. Chem. 277 (2002) 49651–49654.
[26] Y.Y. Hsiao, R.C. Van, H.H. Hung, R.L. Pan, Diethylpyrocarbonate inhibition of H^+-pyrophosphatase possibly involves a histidine residue, J. Protein Chem. 21 (2002) 51–58.
[27] Y.Y. Hsiao, R.C. Van, S.H. Hung, H.H. Lin, R.L. Pan, Roles of histidine residues in plant vacuolar H^+-pyrophosphatase, Biochim. Biophys. Acta 1608 (2004) 190–199.
[28] R.C. Van, Y.J. Pan, S.H. Hsu, Y.T. Huang, Y.Y. Hsiao, R.L. Pan, Role of transmembrane segment 5 of the plant vacuolar H^+-pyrophosphatase, Biochim. Biophys. Acta 1709 (2005) 84–94.
[29] S.Y. Kuo, R.L. Pan, An essential arginyl residue in pyrophosphatase of hypocotyls from etiolated mung beans, Plant Physiol. 93 (1990) 1128–1133.
[30] V. Tuominen, P. Heikinheimo, T. Kajander, T. Torkkel, T. Hyytia, J. Kapyla, R. Lahti, The R78K and D117E active-site variants of *Saccharomyces cerevisiae* soluble inorganic pyrophosphatase: structural studies and mechanistic implications, J. Mol. Biol. 284 (1998) 1565–1580.
[31] A. Schultz, M. Baltscheffsky, Properties of mutated *Rhodospirillum rubrum* H+-pyrophosphatase expressed in *Escherichia coli*, Biochim. Biophys. Acta 1607 (2003) 141–151.
[32] M.J. Buch-Pedersen, M.G. Palmgren, Conserved Asp684 in transmembrane segment M6 of the plant plasma membrane P-type proton pump AHA2 is a molecular determinant of proton translocation, J. Biol. Chem. 278 (2003) 17845–17851.
[33] M. Kawano, K. Igarashi, I. Yamato, Y. Kakinuma, Arginine residue at position 573 in *Enterococcus hirae* vacuolar-type ATPase *Ntp*I subunit plays a crucial role in Na+ translocation, J. Biol. Chem. 277 (2002) 24405–24410.
[34] D. Meredith, Site-directed mutation of Arginine 282 to glutamate uncouples the movement of peptides and protons by the rabbit proton-peptide cotransporter PepT1, J. Biol. Chem. 279 (2004) 15795–15798.
[35] E.J. Kim, R.G. Zhen, P.A. Rea, Heterologous expression of plant vacuolar pyrophosphatase in yeast demonstrates sufficiency of the substrate-binding subunit for proton transport, Proc. Natl. Acad. Sci. U. S. A. 91 (1994) 6128–6132.
[36] R.D. Gietz, R.H. Schiestl, A.R. Willems, R.A. Woods, Studies on the transformation of intact yeast cells by the LiAc/ss-DNA/PEG procedure, Yeast 11 (1995) 355–360.
[37] S. Barik, Site-directed mutagenesis by double polymerase chain reaction: megaprimer method, in: B.A. White (Ed.), Methods Mol. Biol, vol. 15, Humana, New Jersey, 1993, pp. 277–286.
[38] M.M. Bradford, A rapid and sensitive method for the quantitation of microgram quantities of protein utilizing the principle of protein-dye binding, Anal. Biochem. 72 (1976) 248–254.
[39] M.Y. Wang, Y.H. Lin, W.M. Chow, T.P. Chung, R.L. Pan, Purification and characterization of tonoplast ATPase from etiolated mung bean seedlings, Plant Physiol. 90 (1989) 475–481.
[40] U.K. Laemmli, Cleavage of structural proteins during the assembly of the head of bacteriophage T4, Nature 227 (1970) 680–685.
[41] H.H. Lin, Y.J. Pan, S.H. Hsu, R.C. Van, Y.Y. Hsiao, J.H. Chen, R.L. Pan, Deletion mutation analysis on C-terminal domain of plant vacuolar H^+-pyrophosphatase, Arch. Biochem. Biophys. 442 (2005) 206–213.
[42] A.A. Baykov, E.B. Dubnova, N.P. Bakuleva, O.A. Evtushenko, R.G. Zhen, P.A. Rea, Differential sensitivity of membrane-associated pyrophosphatases to inhibition by diphosphonates and fluoride delineates two classes of enzyme, FEBS Lett. 327 (1993) 199–202.
[43] M. Zancani, L.A .Skiera, D. Sanders, Roles of basic residues and salt-bridge interaction in a vacuolar H^+-pumping pyrophosphatase (AVP1) from *Arabidopsis thaliana*, Biochim. Biophys. Acta 1768 (2006) 311–316.